Journal of Zhejiang University-SCIENCE A (Applied Physics & Engineering)
ISSN 1673-565X (Print); ISSN 1862-1775 (Online)
www.zju.edu.cn/jzus; www.springerlink.com
E-mail: jzus@zju.edu.cn

Response of a transmission tower-line system at a canyon site to spatially varying ground motions*

Hong-nan LI[1], Feng-long BAI†‡[1,2], Li TIAN[1], Hong HAO[2]

([1]*State Key Laboratory of Coastal and Offshore Engineering, Dalian University of Technology, Dalian 116024, China*)

([2]*School of Civil and Resource Engineering, University of Western Australia, WA 6009, Australia*)

†E-mail: baifenglong816@163.com

Received Feb. 25, 2010; Revision accepted May 13, 2010; Crosschecked Jan. 5, 2011

Abstract: Collapses of transmission towers were often observed in previous large earthquakes such as the Chi-Chi earthquake in Taiwan and Wenchuan earthquake in Sichuan, China. These collapses were partially caused by the pulling forces from the transmission lines generated from out-of-phase responses of the adjacent towers owing to spatially varying earthquake ground motions. In this paper, a 3D finite element model of the transmission tower-line system is established considering the geometric nonlinearity of transmission lines. The nonlinear responses of the structural system at a canyon site are analyzed subjected to spatially varying ground motions. The spatial variations of ground motion associated with the wave passage, coherency loss, and local site effects are given. The spatially varying ground motions are simulated stochastically based on an empirical coherency loss function and a filtered Tajimi-Kanai power spectral density function. The site effect is considered by a transfer function derived from 1D wave propagation theory. Compared with structural responses calculated using the uniform ground motion and delayed excitations, numerical results indicate that seismic responses of transmission towers and power lines are amplified when considering spatially varying ground motions including site effects. Each factor of ground motion spatial variations has a significant effect on the seismic response of the structure, especially for the local site effect. Therefore, neglecting the earthquake ground motion spatial variations may lead to a substantial underestimation of the response of transmission tower-line system during strong earthquakes. Each effect of ground motion spatial variations should be incorporated in seismic analysis of the structural system.

Key words: Transmission tower-line system, Canyon site, Spatially varying ground motions, Coherency loss, Local site effect
doi:10.1631/jzus.A1000067 **Document code:** A **CLC number:** TU393.3

1 Introduction

As one of the most important components in electricity transmission systems, the high-voltage transmission tower is a significant lifeline structure (Li *et al*., 2005). Until now, most of the research attention on the transmission tower-line system has been paid to the actions of static load, impulsive load, wind load, and ice load (Mozer *et al*., 1977; ASCE, 1982; 1991; Yang *et al*., 1996; Li and Bai, 2006). Only a few studies have considered seismic effect. A transmission tower-line system during its service life, especially those located in a high seismicity region, may be subjected to earthquake loadings. In certain circumstances, the seismic loading effect might be more significant than those from wind or ice load, leading to failure of the structure during strong ground excitations. Collapses of transmission towers have always been observed in previous large earthquakes, such as the Chi-Chi earthquake in Taiwan and the Wenchuan earthquake in Sichuan, China. These collapses were partially attributed to the pulling forces from the transmission lines generated from out-of-phase responses of the adjacent towers owing

‡ Corresponding author

* Project supported by the National Natural Science Foundation of China (No. 50638010), and the Specialized Research Fund for the Doctoral Program of Higher Education of China (No. 20070141036)

to non-uniform earthquake ground motions. Since disruption of the power supply might have catastrophic consequences during the post-earthquake rescue period, and sophisticated structural design to earthquake loads is the key tool for the mitigation of earthquake hazards (Moustafa and Takewaki, 2009), it is very important to understand the responses of coupled transmission tower-line systems to earthquake excitations in order to create a proper design of a system resisting possible earthquake ground motions.

With the rapid development of welding techniques, high strength steel and wire materials and the progress in structural analysis and design theory, the spans and dimensions of transmission tower-line system have increased dramatically. For such a structural system, it is unrealistic to assume that earthquake ground motions at multiple towers are the same because of the inevitable ground motion spatial variations. Many factors cause the ground motion spatial variations, including: (1) the difference in the arrival times of seismic waves at different supports, denoted as the wave passage effect; (2) the coherency loss effect owing to reflections and refractions of the waves in the heterogeneous media of the ground; and (3) the local site effect due to different local soil properties. The seismic response of long span structures subjected to spatially varying earthquake ground motions has attracted the attention of many researchers. Zanardo *et al*. (2002) performed a parametrical study of the pounding effect on responses of a multi-span simply supported bridge with base isolation devices. Hao and Duan (1996) investigated the torsional responses of symmetric buildings subjected to spatially varying base excitations, and studied the effect of spatially varying ground motions on the required separation distance between adjacent building structures to avoid pounding. Rassem *et al*. (1996) studied the effect of multiple support excitations on the response of suspension bridges. Harichandran *et al*. (1996) carried out stationary and transient response analyses of suspension and arch bridges to spatially varying ground motion, and compared the results with responses computed using identical and delayed excitations. Soyluk and Dumanoglu (2000) conducted asynchronous and stochastic dynamic analyses of a cable-stayed bridge considering various wave velocities. Nazmy and Abdel-Ghaffar (1987; 1992) performed the earthquake response analysis of cable-stayed bridges subjected to multi-support as well as uniform seismic excitations. All these investigations concluded that spatially varying earthquake ground motions strongly affect the responses of long span structures. However, most of these studies focus on bridge and building structures, and only linear elastic responses are considered. Owing to complex coupled tower-line vibration and geometric nonlinearity of cable structures, the behaviour of a transmission tower-line system under earthquake ground excitations are expected to be very different from bridge and building structures. Therefore, to better understand the behaviour and to achieve a more reliable design of a transmission tower-line system to resist spatially varying earthquake ground motions, it is necessary to study the responses of such long and complex structures to spatial earthquake ground excitations. Until now, researches on the transmission tower-line system under non-uniform excitations are limited. Yue *et al*. (2006) analyzed the longitudinal response of transmission tower-line system to travelling seismic waves, and concluded that travelling wave input may increase internal force and displacement responses of the structural system. Ghobarah *et al*. (1996) investigated the nonlinear response of overhead power transmission lines to transverse multiple support excitations, in which the effects of wave propagation and the coherency loss of seismic input waves were evaluated, and it was found that ground motion spatial variations had a substantial effect on the structural response. Bai *et al*. (2009) conducted a nonlinear response analysis of a coupled transmission tower-line system to longitudinal spatially varying ground motions, and concluded that ground motion spatial variations might increase the internal force and the displacement response of transmission towers and cables. Note that the local site effects are not taken into consideration in previous studies on seismic responses of long span transmission tower-line systems, in which the sites are assumed to be homogeneous.

In practice, multiple supports of many large dimensional structures may rest on sites of different conditions. Irregular local site conditions will result in different site amplifications and hence affect the structural responses, as observed in the 1995 Kobe earthquake (Kawashima and Unjoh, 1996) and 1999

Chi-Chi earthquake (EERI, 1999). Many studies (Dumanoglu and Soyluk, 2003; Sextos *et al*., 2003a; 2003b; Ates *et al*., 2005) about the site effects on long span structural responses have been reported, and they all concluded that site effects modified the overall behaviour and affected structural responses significantly. Electric power transmission systems generally cover extensive areas with some generating plants at considerable distances from the major demand sites, and a wide variety of local site conditions probably exist (Ang *et al*., 1996). However, studies on the seismic response analysis of long span transmission tower-line system subjected to spatially varying ground motions including the site-response effect cannot be found in previous studies.

The objective of this paper is to investigate the nonlinear responses of a transmission tower-line system at a canyon site subjected to spatially varying ground motions. Detailed numerical simulations are carried out. The effects of ground motion spatial variations induced by wave propagation, coherency loss, and changing site conditions on structural responses are comprehensively analyzed. In this study, the spatial ground motions at a canyon site are simulated stochastically based on an empirical coherency loss function and a filtered Tajimi-Kanai power spectral density function. Site-response effect, which filters the incoming seismic waves and hence changes their amplitudes and frequency contents, is considered here by a transfer function derived from 1D wave propagation theory. The results obtained provide useful information and suggestions for the practical design of long span transmission tower-line systems, and highlight the importance of considering the ground motion spatial variations in the large structural response analysis and design.

2 Model of the transmission tower-line system

In this study, the computer software SAP2000 (Computers and Structures, Inc., USA) is used to analyze the seismic behaviour of the transmission tower-line system with coupled towers and cable components to spatial ground motion excitations. The 3D model of a coupled transmission tower-line system is established based on a real electric power transmission project in the northeast of China. The single tower model is shown in Fig. 1. The weight of the tower is approximately 3×10^4 kg. The structural members of the tower are made of angle steel with the elastic modulus of 206 GPa. It is modeled by 1883 space beam elements with 727 nodes. The connections of members are assumed to be rigid, and the structural supports of the towers are assumed to be fixed. The first frequency of a standalone tower is 1.771 Hz.

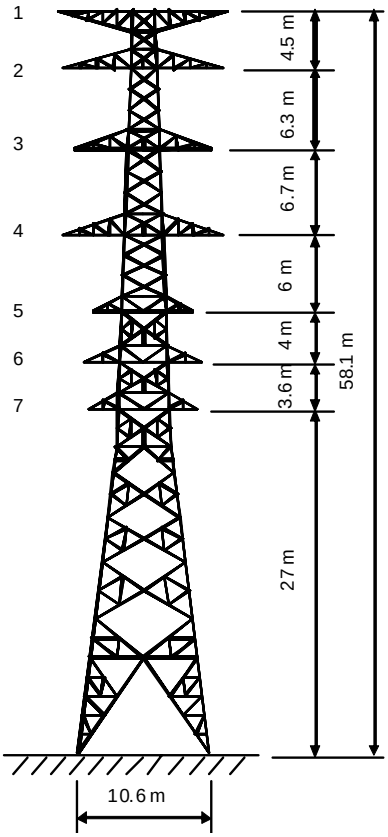

Fig. 1 Transmission tower model
1–7: layer of tower cross arm

There are 28 transmission lines including 24 transmission conductors and 4 ground wires. Only two spans with three towers as shown in Fig. 2 are considered in this study. This simplification may lead to overestimation of the tower responses because it neglects the possible pulling forces from other adjacent spans, which may reduce the overall pulling forces on the side towers under consideration. The separation distance between two towers is 300 m. The transmission conductor is made of aluminium cable with steel reinforcement. The type of transmission

conductor and ground wire are LGJ-630/45 and JL/LB1A-95/55, respectively. Each transmission line is modeled by 300 two-node isoparametric cable elements with three translational degrees of freedom (DOFs) at each node. The initial axial force and large deformation effect of cable are considered. A cable is subjected to vertical uniformly distributed gravity loads and its spatial configuration is a catenary. Based on the coordinate system illustrated in Fig. 3, the initial geometry of the cable profile is defined as (Shen *et al*., 1997)

$$z=\frac{H}{q}\left|\cosh\alpha-\cosh\left|\frac{2\beta x}{l}-\alpha\right|\right|, \tag{1}$$

where

$$\alpha=\sinh^{-1}\left|\frac{\beta c/l}{\sin\beta}\right|+\beta,\quad \beta=\frac{ql}{2H}, \tag{2}$$

where H represents the initial horizontal tension, which can be obtained from a preliminary static analysis, q denotes the uniformly distributed gravity loads along the transmission line, and c and l are the height difference and the horizontal separation distance of two line supports, respectively. The first frequency of the coupled transmission tower-line system is 0.159 Hz, which corresponds to the lateral vibration mode of the top layer cables.

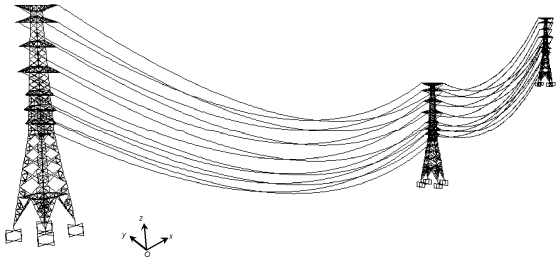

Fig. 2 3D model analysed in this study

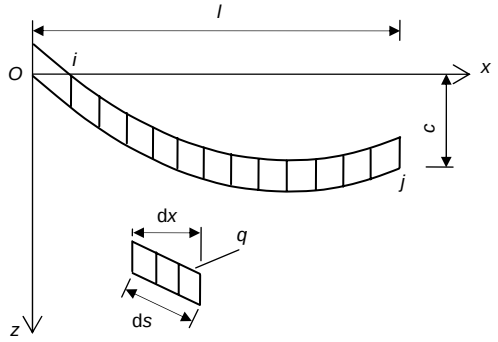

Fig. 3 Coordinate of a single line subjected to vertical uniformly distributed gravity loads

Fig. 4 shows the schematic view of the example transmission tower-line system at a canyon site. Because of the relatively small dimensions of the tower base, the four supports of each tower as shown in Fig. 2 are assumed to experience the same ground excitations. In numerical calculations, geometric nonlinearity of the cables is considered, but material nonlinearity of the structural system is neglected. Because the primary objective is to investigate the effects of ground motion spatial variations on the seismic response of transmission tower-line system, the soil-structure interaction is not considered in this study.

3 Equations of motion

Considering the differential earthquake motions at different tower supports, the equilibrium equation of motion can be written as

$$\begin{bmatrix}\boldsymbol{M}_{ss} & \boldsymbol{M}_{sb}\\ \boldsymbol{M}_{sb}^{T} & \boldsymbol{M}_{bb}\end{bmatrix}\begin{bmatrix}\ddot{\boldsymbol{X}}_{s}\\ \ddot{\boldsymbol{X}}_{b}\end{bmatrix}+\begin{bmatrix}\boldsymbol{C}_{ss} & \boldsymbol{C}_{sb}\\ \boldsymbol{C}_{sb}^{T} & \boldsymbol{C}_{bb}\end{bmatrix}\begin{bmatrix}\dot{\boldsymbol{X}}_{s}\\ \dot{\boldsymbol{X}}_{b}\end{bmatrix}+\begin{bmatrix}\boldsymbol{K}_{ss} & \boldsymbol{K}_{sb}\\ \boldsymbol{K}_{sb}^{T} & \boldsymbol{K}_{bb}\end{bmatrix}\begin{bmatrix}\boldsymbol{X}_{s}\\ \boldsymbol{X}_{b}\end{bmatrix}=\begin{Bmatrix}0\\ \boldsymbol{P}_{b}\end{Bmatrix}, \tag{3}$$

where $\boldsymbol{M}$, $\boldsymbol{C}$, and $\boldsymbol{K}$ are the mass matrix, the viscous damping matrix, and the stiffness matrix, respectively. The subscripts 'ss', 'bb', and 'sb' denote the structural DOFs, the support DOFs, and the coupled DOFs, respectively. $\ddot{\boldsymbol{X}}$, $\dot{\boldsymbol{X}}$, and $\boldsymbol{X}$ are the acceleration vector, velocity vector, and displacement vector, respectively. $\boldsymbol{P}$ represents the supporting force vector. The subscripts 's' and 'b' refer to the structure and the base, respectively.

From Eq. (3), the equilibrium equation defining the response DOFs of superstructure can be derived as

$$\begin{aligned}&\boldsymbol{M}_{ss}\ddot{\boldsymbol{X}}_{s}+\boldsymbol{C}_{ss}\dot{\boldsymbol{X}}_{s}+\boldsymbol{K}_{ss}\boldsymbol{X}_{s}\\ &=-\boldsymbol{M}_{sb}\ddot{\boldsymbol{X}}_{b}-\boldsymbol{C}_{sb}\dot{\boldsymbol{X}}_{b}-\boldsymbol{K}_{sb}\boldsymbol{X}_{b}.\end{aligned} \tag{4}$$

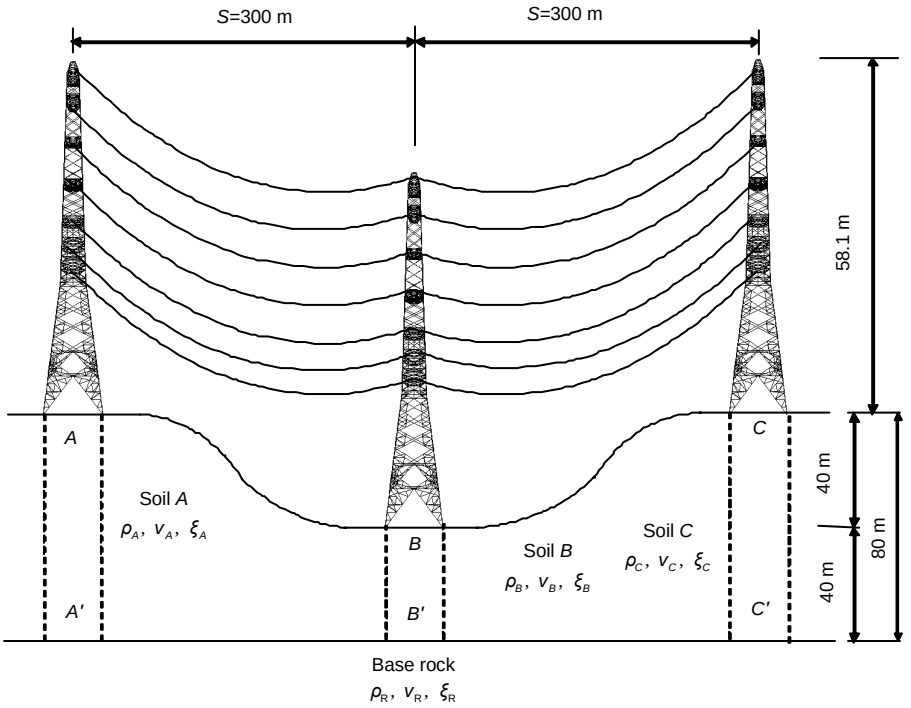

Fig. 4 Schematic view of the transmission tower-line system at a canyon site

Points *A*, *B*, and *C* represent the locations of the three towers on the ground surface, the corresponding points on the base rock are *A*′, *B*′ and *C*′; *h*, *S*, and *H* represent the height of the tower, the horizontal span between the adjacent towers, and the depth of the soil layer, respectively; ρ_R, v_R, and ξ_R denote the density, the shear wave velocity, and the damping ratio of the base rock, respectively, and the corresponding parameters of the soil layer under the support point *e* (*e* represents point *A*, *B*, or *C*) are ρ_e, v_e, and ξ_e, respectively

Assuming the lumped mass and neglecting the cross damping coefficients between the structure and the base DOFs, we can obtain $\boldsymbol{M}_{sb}=0$ and $\boldsymbol{C}_{sb}=0$. Then Eq. (4) is reduced to

$$\boldsymbol{M}_{ss}\ddot{\boldsymbol{X}}_s+\boldsymbol{C}_{ss}\dot{\boldsymbol{X}}_s+\boldsymbol{K}_{ss}\boldsymbol{X}_s=-\boldsymbol{K}_{sb}\boldsymbol{X}_b. \quad (5)$$

In this study, spatially varying ground displacement time histories at multiple supports, $\boldsymbol{X}_b$, is simulated, and used as an input to calculate structural responses. To use ground displacement as an input, a spring with a large stiffness needs to be added in the direction of ground displacement. This ensures essentially zero relative displacement between structural supports and ground. The commercial computer program SAP2000 automatically assigns the spring stiffness for analysis with spatially varying ground displacement input, and the dynamic load in the direction of input displacement equal to the spring stiffness is multiplied by the input displacement of the tower support.

4 Simulation of spatially varying ground motions

4.1 Power spectral density function

The power spectral density function of ground acceleration characterizes the earthquake ground motion amplitude and frequency contents. Ground motion intensities at *A*′, *B*′, and *C*′ on the base rock are assumed to be the same. The power spectral density is modeled by a filtered Tajimi-Kanai power spectral density function (Ruiz and Penzien, 1969):

$$S_g(\omega)=\left|H_p(i\omega)\right|^2 S_0(\omega), \quad (6)$$

where

$$\left|H_p(i\omega)\right|^2=\frac{\omega^4}{(\omega_f^2-\omega^2)^2+(2\omega_f\omega\xi_f)^2} \quad (7)$$

is a high pass filter function, which can filter out ground acceleration energy at very low frequencies to eliminate drifting of ground velocity and

displacement. ω_f and ξ_f are the central frequency and damping ratio of the high pass filter, respectively. $S_0(\omega)$ is the Tajimi-Kanai power spectral density function (Tajimi, 1960), which is given by

$$S_0(\omega)=\frac{1+4\xi_g^2\omega^2/\omega_g^2}{(1-\omega^2/\omega_g^2)^2+4\xi_g^2\omega^2/\omega_g^2}\Gamma, \quad (8)$$

where ω_g and ξ_g are the central frequency and damping ratio of the Tajimi-Kanai power spectral density function, respectively, and both of them depend on the site conditions, epicentral distance, and earthquake magnitude; Γ is a scale factor depending on the ground motion intensity, and Γ=0.0078 m^2/s^3 is used in this study, which corresponds to a ground acceleration of duration T=20 s and the peak value (PGA) 0.3g (Der Kiureghian, 1980). Without losing generality, in this study, it is assumed that $f_f=\omega_f/(2\pi)$=0.25 Hz, ξ_f=0.6, $f_g=\omega_g/(2\pi)$=5.0 Hz, and ξ_g=0.6. Fig. 5 shows the power spectral density functions of the ground acceleration and displacement ($S_d=S_g/\omega^4$) on the base rock.

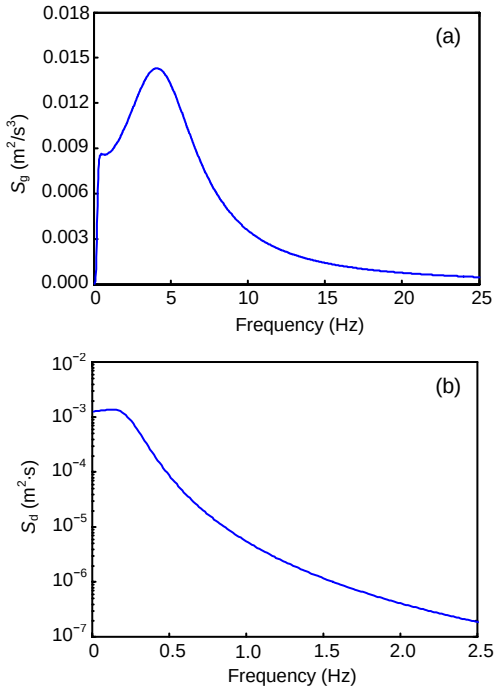

Fig. 5 Filtered power spectral density function on base rock
(a) Acceleration; (b) Displacement

4.2 Coherency loss function

An empirical coherency loss function derived from recorded strong ground motions at the smart-1 array is used in this study to model ground motion coherency loss (Hao *et al.*, 1989). The coherency loss function between two locations i' and j' on the base rock is

$$\left|\gamma_{i'j'}(i\omega,d_{i'j'})\right|=\exp(-\beta d_{i'j'})\exp\left[-\alpha(\omega)\sqrt{d_{i'j'}}(\omega/(2\pi))^2\right], \quad (9)$$

where $d_{i'j'}$ is the projected distance between points i' and j' in the wave propagation direction, β is a constant and $\alpha(\omega)$ is a function with the form:

$$\alpha(\omega)=\begin{cases}2\pi a/\omega+b\omega/(2\pi)+c,\\ \quad 0.314\text{ rad/s}\le\omega\le 62.83\text{ rad/s},\\ 0.1a+10b+c, \quad \omega>62.83\text{ rad/s},\end{cases} \quad (10)$$

where a, b, and c are constants and can be obtained by the regression method. The constants of the coherency loss function used here are derived from the recorded strong motions during Event 45 at the smart-1 array (Hao, 1989), which represents highly correlated ground motions. For comparison, two modified coherency loss functions are also applied in this study, which represent intermediately and weakly correlated ground motions, respectively. Table 1 gives the constants of the coherency loss function corresponding to the three correlated ground motions.

Table 1 Parameters for coherency loss functions

Coherency	β ($\times10^{-4}$)	a ($\times10^{-4}$)	b ($\times10^{-4}$)	c ($\times10^{-4}$)
Highly	1.109	38.53	−0.181	1.177
Intermediately	3.507	113.3	−0.181	1.177
Weakly	11.09	385.3	−0.181	1.177

It should be noted that the above coherency loss function was derived from the recorded strong motions on the ground surface at the smart-1 array. There is no general consent yet on how the ground motion spatial variation on the base rock should be modeled. However, in this study, the soil layer between the tower support and the base rock is modeled as a homogeneous medium, as shown in Fig. 4, which will

only affect the ground motion intensity and phase delay, and the ground motion coherency loss will not be changed. Therefore, the coherency loss function described above is suitable to model the coherency loss on the base rock in this study without losing accuracy to any great extent. Note that the coherency loss function will be changed if the soil site is modeled as a heterogeneous medium with varying properties, in which this aspect of the problem is beyond the scope of the present work.

The cross power spectral density function of motions at two locations i' and j' on the base rock is expressed as

$$S_{i'j'}(i\omega)=S_{\mathrm{g}}(\omega)\gamma_{i'j'}(i\omega), \tag{11}$$

where

$$\gamma_{i'j'}(i\omega)=\left|\gamma_{i'j'}(i\omega)\right|\exp(-i\omega d_{i'j'}/v_{\mathrm{app}}), \tag{12}$$

where v_{app} is the apparent wave propagation velocity and the exponential function represents the influence of the wave passage effect.

4.3 Site effect

The base rock is assumed to be homogenous, but the material properties of topsoil with large distances are different. These can always be found at an alluvial valley due to the irregular site effect. Thereby, the ground surface motions would be different due to the variation in the filtering and amplification effects of the soil layer under the structural supports. The site effect can be represented by a frequency-dependent transfer function. Here, the transfer function of ground motion due to wave propagation from the base rock point i' to the ground surface point i is based on 1D wave propagation assumption, which is expressed as (Hao and Chouw, 2006)

$$H_i(i\omega)=\frac{(1+r_i-i\xi_i)\mathrm{e}^{-i\omega\tau_i(1-2i\xi_i)}}{1+(r_i-i\xi_i)\mathrm{e}^{-2i\omega\tau_i(1-2i\xi_i)}}, \tag{13}$$

where $\tau_i=h_i/v_i$ is the wave propagation time from point i' to i, and the reflection coefficient for up-going waves r_i, which plays a significant role in the effects of the soil layer, is given by

$$r_i=\frac{\rho_{\mathrm{R}}v_{\mathrm{R}}-\rho_i v_i}{\rho_{\mathrm{R}}v_{\mathrm{R}}+\rho_i v_i}. \tag{14}$$

Table 2 gives the corresponding parameters of different site conditions. The auto power spectral density function at ground surface point i can be obtained by

$$S_{ii}(\omega)=\left|H_i(i\omega)\right|^2 S_{\mathrm{g}}(\omega), \tag{15}$$

and the cross power spectral density function between points i and j is given by

$$\begin{aligned}S_{ij}(i\omega)&=H_i(i\omega)H_j^*(i\omega)S_{i'j'}(i\omega)\\&=H_i(i\omega)H_j^*(i\omega)\gamma_{i'j'}(i\omega)S_{\mathrm{g}}(\omega),\end{aligned} \tag{16}$$

where the superscript '*' denotes the complex conjugate.

Table 2 Parameters of local site conditions

Type	Density (kg/m^3)	Wave velocity (m/s)	Damping ratio
Base rock	3000	1500	0.05
Firm soil	2000	450	0.05
Medium soil	1500	300	0.05
Soft soil	1500	200	0.05

4.4 Method for generating spatially varying ground motions

The spatially varying ground motions are simulated using the above empirical coherency loss function and the derived spatial ground motion power spectral density function, which is based on the simulation method performed by Hao *et al.* (1989). The ground acceleration power spectral density function of the site with three structural supports can be expressed as

$$\boldsymbol{S}(i\omega)=\begin{bmatrix}S_{11}(\omega) & S_{12}(i\omega) & S_{13}(i\omega)\\ S_{21}(i\omega) & S_{22}(\omega) & S_{23}(i\omega)\\ S_{31}(i\omega) & S_{32}(i\omega) & S_{33}(\omega)\end{bmatrix}, \tag{17}$$

where $S_{ii}(\omega)$ and $S_{ij}(i\omega)$ (i, j=1, 2, 3) are defined in Eqs. (15) and (16), respectively. Since the matrix $\boldsymbol{S}(i\omega)$ is positive definite and Hermitian, it can be decomposed into the multiplication of a complex lower triangular matrix $\boldsymbol{L}(i\omega)$ and its Hermitian matrix $\boldsymbol{L}^{\mathrm{H}}(i\omega)$ by Cholesky's method, which is given by

$$\boldsymbol{S}(i\omega)=\boldsymbol{L}(i\omega)\boldsymbol{L}^{\mathrm{H}}(i\omega). \tag{18}$$

The matrix $\boldsymbol{L}(i\omega)$ is defined as

$$\boldsymbol{L}(i\omega)=\begin{bmatrix} L_{11}(\omega) & 0 & 0 \\ L_{21}(i\omega) & L_{22}(\omega) & 0 \\ L_{31}(i\omega) & L_{32}(i\omega) & L_{33}(\omega) \end{bmatrix}, \tag{19}$$

where

$$\begin{aligned} L_{ii}(\omega)&=\left[S_{ii}(\omega)-\sum_{k=1}^{i-1}S_{ik}(i\omega)S_{ik}^{*}(i\omega)\right]^{1/2},\ i=1,2,3,\\ L_{ij}(i\omega)&=\frac{S_{ij}(i\omega)-\sum_{k=1}^{i-1}S_{ik}(i\omega)S_{jk}^{*}(i\omega)}{S_{jj}(\omega)},\quad j=1,2,\cdots,i, \end{aligned} \tag{20}$$

where the superscript '*' denotes a complex conjugate of a complex number. The spatial ground motion time histories of the three different locations can be obtained by

$$u_k(t)=\sum_{m=1}^{n}\sum_{l=1}^{N}A_{km}(\omega_l)\cos[\omega_l t+\theta_{km}(\omega_l)+\varphi_{ml}(\omega_l)], \tag{21}$$

where $\omega_l=l\Delta\omega$, and $\Delta\omega=\omega_N/N$. n represents the total number of support points, and m is the support point number. N denotes the total number of the discrete frequency, and l is the point number of discrete frequency. k=1, 2, and 3, representing the support points A, B, and C in this study. ω_N represents an upper cut-off frequency. $\varphi_{ml}(\omega_l)$ is a random phase angle uniformly distributed over the range 0 to 2π, and $\varphi_{rs}(\omega_s)$ is another random phase angle corresponding to the support point number r and the discrete frequency number s. φ_{ml} and φ_{rs} should be statistically independent unless $m=r$ and $l=s$. $A_{km}(\omega_l)$ and $\theta_{km}(\omega_l)$ denote the amplitudes and phase angles of the generated time histories, which ensure the spectrum of time histories compatible with those given in Eq. (17), and can be estimated by

$$\begin{aligned} A_{km}(\omega_l)&=\sqrt{4\Delta\omega}\left|L_{km}(i\omega_l)\right|,\\ \theta_{km}(\omega_l)&=\arctan\frac{\mathrm{Im}[L_{km}(i\omega_l)]}{\mathrm{Re}[L_{km}(i\omega_l)]}. \end{aligned} \tag{22}$$

Note that earthquake ground motions are non-stationary processes. The non-stationary ground motion time histories at different locations can be obtained by multiplying each corresponding stationary time series with an appropriate shape function

$$f_k(t)=\zeta(t)u_k(t),\ k=1,2,3, \tag{23}$$

where the shape function $\zeta(t)$ is of the following form (Jennings *et al*., 1968)

$$\zeta(t)=\begin{cases} (t/t_0)^2, & 0\le t\le t_0 \\ 1, & t_0<t\le t_n, \\ \exp[-0.155(t-t_n)], & t_n<t, \end{cases} \tag{24}$$

where t_0 and t_n denote the initial time and the end time of the stationary segment in dominant earthquake vibration, respectively, with t_0=2 s and t_n=10 s.

In this study, the ground motion duration is assumed to be 20 s, the simulation is carried out with a sampling frequency of 50 Hz and the upper cut-off frequency is set to 25 Hz. To improve the computational efficiency, the ground motions are generated in the frequency domain using the fast fourier transform technique, with a total number of points N=1024 for each simulated time history.

A total of 11 cases, representing different spatial variations as described in Table 3, of spatial ground motions are simulated. In each case, three horizontal ground motion time histories are simulated corresponding to the spatial ground motions at the three tower supports that are at distances of 0, 300, and 600 m. Figs. 6–9 show some typical sets of simulated spatial horizontal accelerations and displacement time histories on uniform and non-uniform sites with the apparent velocity of 1000 m/s and are highly correlated.

Figs. 10 and 11 show the comparison of the coherency loss between the typical simulated ground accelerations on the uniform and non-uniform sites and the corresponding empirical coherency losses. The simulated ground motions are compatible with the same empirical coherency loss function regardless of local site conditions, which again verifies that the non-uniform site with the homogeneous medium soil sets does not change the ground motion coherency

Table 3 Seismic excitation cases

Case	Wave apparent velocity (m/s)	Coherency	Site condition		
			Support *A*	Support *B*	Support *C*
1	Infinite	Perfectly	Firm	Firm	Firm
2	1000	Perfectly	Firm	Firm	Firm
3	Infinite	Highly	Firm	Firm	Firm
4	1000	Highly	Firm	Firm	Firm
5	1000	Highly	Medium	Firm	Medium
6	500	Highly	Firm	Firm	Firm
7	2000	Highly	Firm	Firm	Firm
8	1000	Intermediately	Firm	Firm	Firm
9	1000	Weakly	Firm	Firm	Firm
10	1000	Highly	Soft	Firm	Soft
11	1000	Highly	Soft	Medium	Soft

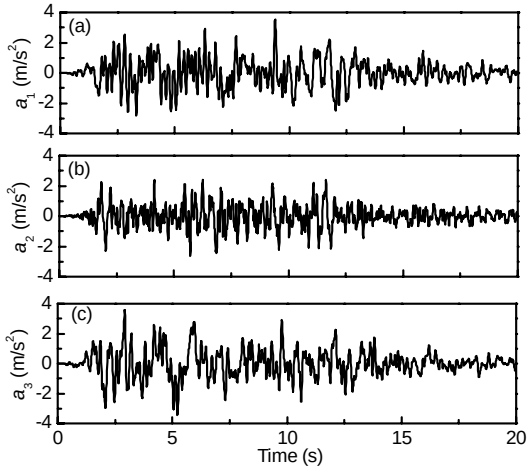

Fig. 6 Generated spatially correlated ground accelerations on a uniform firm site (case 4)
(a) Support *A*; (b) Support *B*; (c) Support *C*

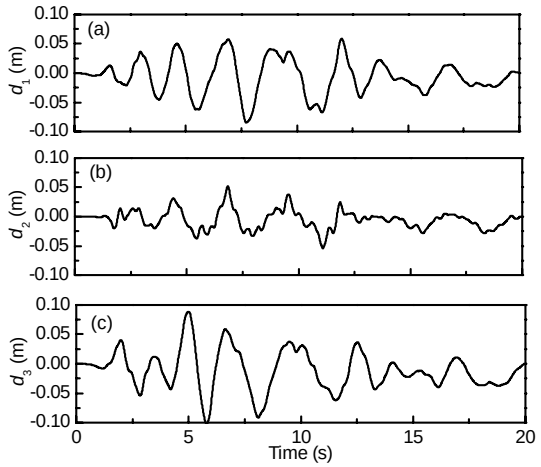

Fig. 7 Generated spatially correlated ground displacements on a uniform firm site (case 4)
(a) Support *A*; (b) Support *B*; (c) Support *C*

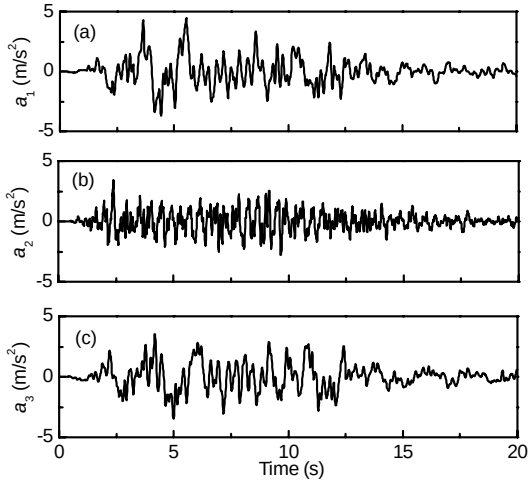

Fig. 8 Generated spatially correlated ground accelerations on a soft-firm-soft site (case 10)
(a) Support *A*; (b) Support *B*; (c) Support *C*

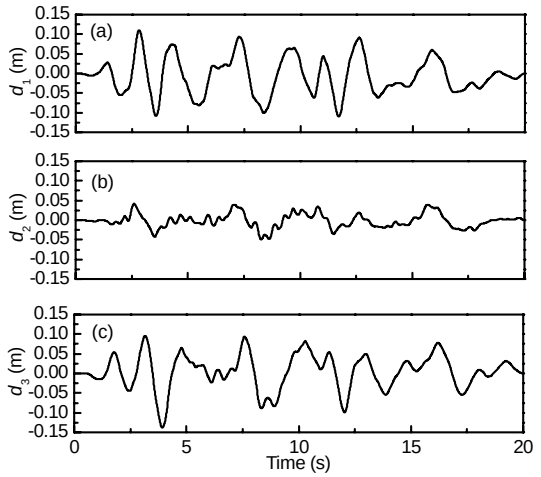

Fig. 9 Generated spatially correlated ground displacements on a soft-firm-soft site (case 10)
(a) Support *A*; (b) Support *B*; (c) Support *C*

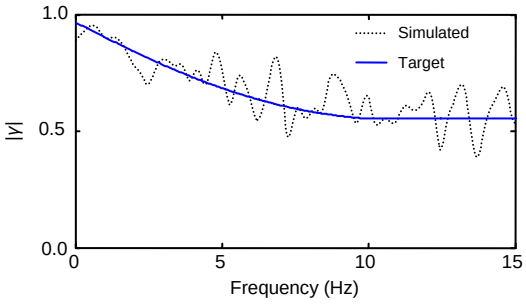

Fig. 10 Model and typical coherency loss function of simulated motions at supports *B* and *C* on a firm-firm site

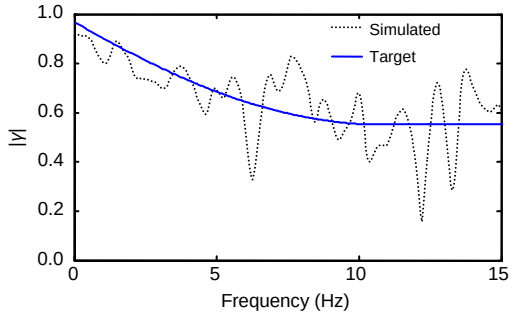

Fig. 11 Model and typical coherency loss function of simulated motions at supports *B* and *C* on a firm-soft site

loss even though the local site effect exists. It can also be noted that when the site is uniform, the ground motions at the three support points are similar because the spatial variations are induced only by wave passage effect and coherency loss effect. When the site is non-uniform, the difference between the ground motion time histories at the three support points is more prominent because different local site amplifications also contribute to the ground motion spatial variations. Compared with the ground motions on a firm site, those on a soft soil site have more pronounced low frequency contents. Thus, the ground motion on a soft soil site has larger peak ground displacement than that on a firm site as shown in Fig. 9. This will generate different quasi-static responses of spatial structures.

5 Numerical analysis

Nonlinear responses of the coupled transmission tower-line system (Fig. 4) subjected to the above simulated spatially varying ground motions are calculated. The direction of the apparent seismic wave propagation is assumed to coincide with the longitudinal direction of the structural system. The commercial computer software SAP2000 is used. The mass of the model is based on the lumped mass concept at the node joint. The damping ratio of the tower and the cable are assumed to be 2% and 1% for all modes, respectively. The Newmark-β method is applied in the numerical integration, where β is set to 0.25. For each ground motion case listed in Table 3, independent numerical calculations are carried out using five sets of independently simulated spatial ground motions as input. Ensemble mean value and standard deviation of each response quantity are obtained from the five numerical calculation results. Since the standard deviations are much smaller than the corresponding mean values, only the mean response values corresponding to the middle tower and the transmission lines of the second span are presented and discussed.

5.1 Effect of ground motion spatial variations

For long span structures, seismic ground motion spatial variation at multiple structural supports is inevitable. However, because of the lack of ground motion spatial variation information, in most analyses and designs of long span structures to resist earthquake loadings, the assumptions of uniform ground motions, or spatial ground motions with only wave passage effect are often adopted. In this section, the effects of seismic ground motion spatial variations on the responses of the long span transmission tower-line system are comprehensively examined. Responses of the structural model to the first 5 cases of simulated ground motions are calculated. Besides the ground motion spatial variation effect due to seismic waves propagating vertically in different depth homogenous soil layer, case 1 is for neglecting ground motion spatial variation on the firm site, case 2 considering spatial ground motions on the firm site with wave passage effect only, case 3 considering spatial ground motions on the firm site with coherency loss effect only, and case 4 considering spatial ground motions on the firm site with both wave passage effect and coherency loss effect. Moreover, owing to the heterogeneous site conditions, case 5 is for considering spatial ground motions induced by wave passage and

coherency loss effect, as well as the local site effect. Therefore, the significance of ground motion spatial variations generally increases from case 1 to case 5.

5.1.1 Seismic response of transmission lines

As shown in Fig. 12, with the seismic input hardly considering ground motion spatial variation (case 1), the responses of cable displacement are exactly symmetric, indicating that the antisymmetric modes are slightly excited. When spatially varying ground motions are considered, the antisymmetric vibration modes will be excited. The contributions from the antisymmetric modes are prominent. The more significant the ground motion spatial variation, the larger the cable response. Case 5 ground motions, which have most significant spatial variations, produce the largest cable displacement equals 118.7 cm at one-third span of the transmission line, followed by case 4 ground motions. Considering spatial ground motion wave passage effect only (case 2) results in larger responses than mainly considering the spatial ground motion coherency loss effect (case 3), indicating that the ground motion wave passage effect is more significant than the coherency loss effect for this structural system. Hao (1993) revealed that the spatial ground motion wave passage effect is more significant if the structure is relatively flexible as compared to the dominant ground motion frequency and its responses are governed by dynamic responses, while spatial ground motion coherency loss effect becomes more pronounced if the structure is relatively stiff and its responses are governed by quasi-static responses. The coupled transmission tower-line system under consideration consists of high towers and long flexible cables, which makes it a dramatically flexible structure. Therefore, the ground motion wave passage effect is more significant than the coherency loss effect. Similar results can be observed in Fig. 13, as the axial force responses in each layer cable obtained from case 2 and case 4 are close to each other. It is also obvious that the more significant the ground motion spatial variation, the larger the axial force responses in the cables. The largest axial force equals 21.2 kN in the second layer cable corresponding to the response under ground motion excitations of case 5, which requires special attention in the seismic design of transmission lines. Note that the axial force response in the top layer cable is the minimum, and the effect of ground motion spatial variation on it is smaller than those on the other layer cables. This is because the top layer cables are ground wires, their cross-section dimension and mass are smaller than these of the transmission conductors, and thus the influences of inertial effect owing to their self-weight and the coupling effects are insignificant.

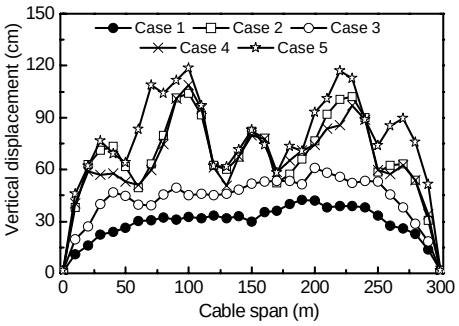

Fig. 12 Mean maximum vertical cable displacements in the second layer induced by the first 5 cases of ground excitations

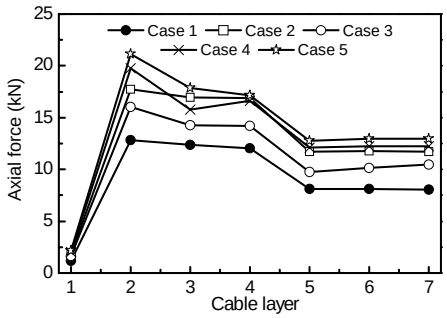

Fig. 13 Mean maximum cable axial forces induced by the first 5 cases of ground excitations

5.1.2 Seismic response of transmission towers

Fig. 14 shows the mean maximum axial forces in tower members along the height of the middle tower corresponding to the first 5 cases of spatial ground excitations. The axial force responses corresponding to case 1 are approximately the same as those obtained from case 3, which indicates that the coherency loss effect on the axial force responses of the tower is not significant. Differing from the seismic response of the transmission line, the axial force responses of the tower considering the wave passage effect only (case 2) are larger than those considering spatial ground motions with both wave passage effect and coherency loss effect. As can be noticed, neglecting ground motion spatial variations, the axial force

responses in the tower members could be substantially underestimated, especially in those members in the lower half of the middle tower, the axial forces could be underestimated by more than 35%.

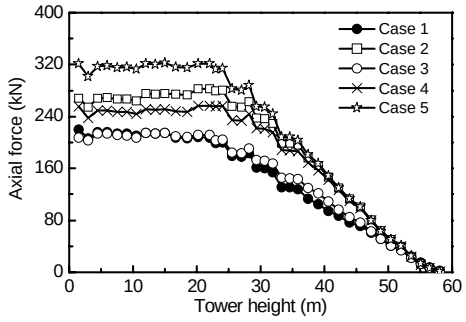

Fig. 14 Mean maximum axial forces in tower members induced by the first 5 cases of ground excitations

The mean maximum longitudinal displacements of cross arms in the middle tower corresponding to the first 5 cases of spatial ground excitations are shown in Table 4. As expected, the longitudinal displacements of cross arms in each case are amplified gradually with the increase of their location heights, which is due to the whiplash effect. In general, the higher the cross arm, the larger the effect of ground motion spatial variation. The largest longitudinal displacement of the top cross arm is 14.66 cm, which is associated with the ground motion excitations of case 5. On the other hand, in terms of a large dimensional transmission tower, the longitudinal displacements in the cross arms are extremely small, and the displacement increments in tower are not significant when considering ground motion spatial variations. Therefore, the displacement responses of tower cross arms are not presented and discussed hereafter for brevity.

Table 4 Mean maximum longitudinal displacements of the tower cross arms under different ground excitations

Layer	Mean maximum longitudinal displacement (cm)				
	Case 1	Case 2	Case 3	Case 4	Case 5
1	9.91	13.34	11.31	12.92	14.66
2	9.40	12.32	10.52	12.03	13.14
3	8.88	10.84	9.67	10.74	11.43
4	8.37	9.53	8.96	9.53	10.10
5	7.95	8.61	8.43	8.65	9.27
6	7.69	8.08	7.82	8.21	8.78
7	7.47	7.73	7.62	7.87	8.40

The above analyses have demonstrated the importance of ground motion spatial variation on the response of coupled transmission tower-line system. As discussed above, ground motion spatial variation is induced by the wave passage effect, coherency loss effect, and non-uniform local site effect. In the following, these three effects on ground motion spatial variations are investigated separately in detail to examine their influence on the transmission tower-line system.

5.2 Spatial ground motion wave passage effect

Wave propagation will cause a phase delay between spatial ground motions. The phase delay depends on the separation distance and the wave propagation apparent velocity. The wave apparent velocity is the projected velocity in the horizontal direction along the wave propagation direction. Thus, the apparent velocity will be infinite (upper limit) if the seismic wave propagates vertically and there is no phase delay between motions at any two points on the ground surface. Or it will be equal to the shear wave propagation velocity of the site (lower limit) if the seismic wave propagates horizontally. The previous study revealed that the wave propagation apparent velocity is also frequency dependent and quite irregular (Hao, 1989). There is no general consent yet on how the apparent velocity should be modeled. In this study, constant apparent velocities are assumed as most previous studies did. Without losing generality, four different wave apparent velocities v_{app} of 500 m/s (case 6), 1000 m/s (case 4), 2000 m/s (case 7), and infinite (case 3) are considered, which covers the possible range of practical apparent seismic wave propagation velocities in a firm soil site. In all these cases, spatial ground motions are assumed to be highly correlated, and all the three tower supports are sited on a homogenous firm site. Therefore, the only difference amongst these spatial ground motion cases is the phase delay between motions at the three tower supports.

5.2.1 Seismic response of transmission lines

As shown in Figs. 15 and 16, increasing the spatial ground motion phase delay, i.e., reducing the seismic wave apparent velocity from the infinite

(case 3) to 2000 m/s (case 7), 1000 m/s (case 4), and 500 m/s (case 6) generally results in the increases of the vertical displacements and axial forces in transmission lines, indicating that the structural system is sensitive to earthquake ground motion phase delay. In general, the more significant the phase delay between the spatial ground motions, the larger the cable response. The largest cable displacement is about 140 cm at one-third span of the transmission line, which is induced by spatial ground motions with the lowest wave velocity (500 m/s) (Fig. 15). Although assuming ground motions with low wave velocities in general leads to a conservative estimation of the cable responses, it may also result in some underestimation of the axial force responses in the lower layer cables (Fig. 16). Hence, an accurate estimation of the wave apparent velocity of the site where the tower located is essential to the seismic design of transmission lines.

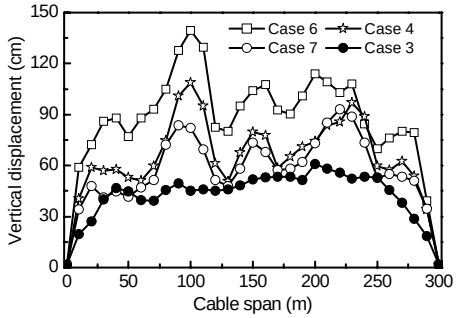

Fig. 15 Mean maximum vertical cable displacements in the second layer induced by motions with different wave velocities

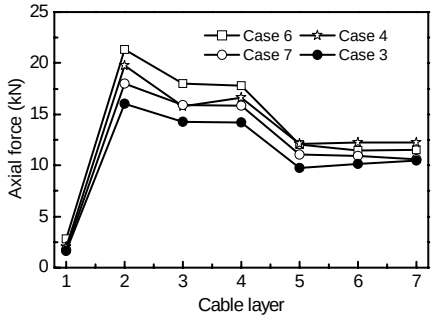

Fig. 16 Mean maximum cable axial forces induced by motions with different wave velocities

5.2.2 Seismic response of transmission towers

Fig. 17 shows the mean maximum axial forces in tower members along the height of the middle tower induced by spatial ground motions with different apparent wave velocities. Similar to the seismic responses of the transmission line, case 6 with the lowest velocity (500 m/s) results in the largest axial force responses of tower members, followed by case 4 (1000 m/s) ground motions. It is interesting to note that the axial force responses induced by case 3 with the infinite wave velocity could be overestimated by 10% compared with those to spatial ground motions with the wave velocities of 2000 m/s (case 7), which also indicates that the transmission tower is sensitive to the ground motion phase difference.

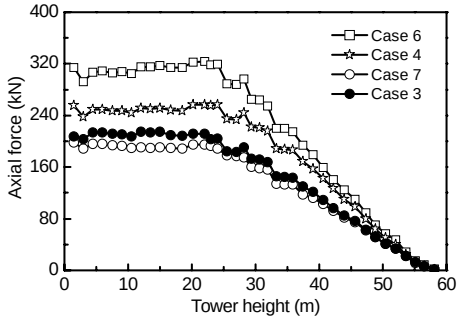

Fig. 17 Mean maximum axial forces in tower members induced by motions with different wave velocities

The above results demonstrated that the spatial ground motion phase difference has a significant effect on the structural responses. Neglecting the spatial ground motion phase difference may lead to an erroneous estimation of transmission tower-line responses. As shown in Fig. 17, the mean maximum axial forces in the lower half of the tower could be underestimated by approximately 40% if the spatial ground motion phase differences are neglected. Therefore, to obtain a reliable seismic response analysis of transmission tower-line systems, the spatial ground motion phase difference should be considered.

5.3 Spatial ground motion coherency loss effect

To investigate the coherency loss effect on the response of the coupled transmission tower-line system, four cases of spatial ground motions, i.e., no coherency loss or perfectly correlated (case 2), highly correlated (case 4), intermediately correlated (case 8) and weakly correlated (case 9), are used as seismic inputs to calculate the structural responses. Fig. 18

shows the model cross correlation functions for these four cases in which the parameters are defined in Table 1. Note that, as indicated in Table 3, these four cases of ground motions are generated with the same apparent velocity and the same site conditions. Thus, the only differences are cross correlations between the spatial ground motions.

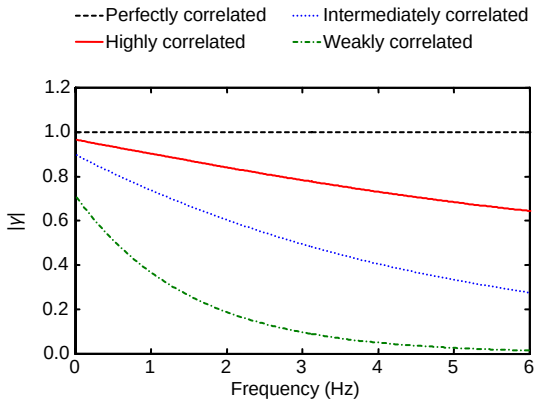

Fig. 18 Different cross correlation functions

5.3.1 Seismic response of transmission lines

As shown in Fig. 19, in general, increasing the coherency loss, or reducing the cross correlation between spatial ground motions, results in the decrease of the responses of cable displacement. However, it is noted that in the considered cases the weakly correlated ground motions cause the largest cable displacements near the mid span. This is because the cable vertical displacements near the mid span will be excited primarily by antisymmetric modes, and the less-correlated multiple horizontal motions excite the cable antisymmetric modes more and the symmetric modes less. The results also reveal that the more the spatial ground motions correlated, the more the responses resemble each other due to a no coherency loss case. On the other hand, the calculated results shown in Fig. 20 indicate that the coherency loss effect on the axial force responses of transmission lines is not significant, and the responses obtained from spatial ground motions with the coherency loss could be larger or smaller than those due to spatial ground motions without the coherency loss.

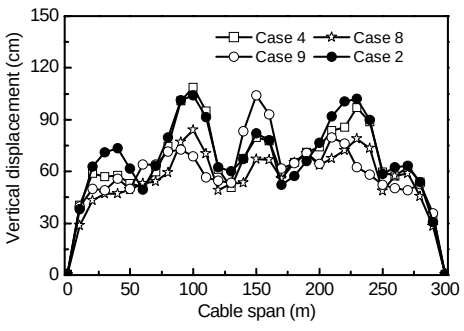

Fig. 19 Mean maximum vertical cable displacements induced by motions with different coherency losses

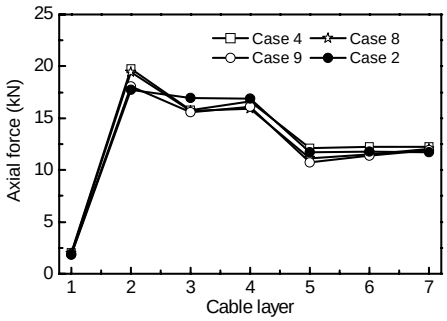

Fig. 20 Mean maximum cable axial forces induced by motions with different coherency losses

5.3.2 Seismic response of transmission towers

Fig. 21 shows the mean maximum axial forces in tower members along the height of the middle tower induced by spatial ground motions with different coherency losses. Besides a slight difference between the responses induced by highly and intermediately correlated ground motions, the axial forces of tower members decrease with the increase of coherency loss (less correlated). If the weakly correlated spatial ground motions are assumed, the generated axial forces in the tower members will be dramatically underestimated. This is because the ground motions in case 9 are almost uncorrelated, and it may reduce the pseudostatic response of the tower.

Although the spatial ground motion without the coherency loss generally results in a conservative estimation of structural responses, it underestimates the seismic responses of transmission tower-line systems in some cases, indicating the effect of coherency loss between ground motions could also be significant, if not more significant than the wave passage effect. Neglecting coherency losses between spatial ground motions may lead to incorrect predictions of structural responses.

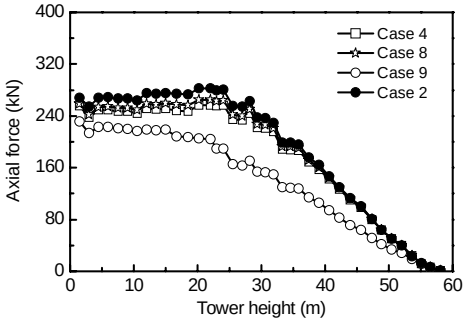

Fig. 21 Mean maximum axial forces in tower members induced by motions with different coherency losses

5.4 Spatial ground motion local site effect

The responses of the structural system to spatial ground motions with four different site conditions are calculated to investigate the effect of different site conditions on ground motion spatial variations and on responses of the transmission tower-line systems. These four site conditions include homogeneous firm site (case 4), heterogeneous site with firm soil on the middle tower support and medium soil on the side tower supports (case 5), heterogeneous site with firm soil on the middle tower support and soft soil on the side tower supports (case 10), and heterogeneous site with medium soil on the middle tower support and soft soil on the side tower supports (case 11). The schematic view of the transmission tower-line system crossing a canyon site is shown in Fig. 4, and the corresponding soil parameters considered in this section are given in Table 2. All these four cases of spatial ground motions have the same apparent velocity and coherency loss. Thus, the only difference between them are the local site conditions. The spatial ground motions corresponding to the heterogeneous site conditions (cases 5, 10, and 11) have additional spatial variations induced by different site conditions besides the phase delay and the loss of coherency.

5.4.1 Seismic response of transmission lines

Fig. 22 illustrates the mean maximum vertical displacements of a cable in the second layer. The mean maximum axial forces in cables of each layer are plotted in Fig. 23. The results indicate the importance in considering the possible varying site conditions in analysis and design of transmission lines to earthquake ground motions. The assumption of uniform site condition simplification may lead to incorrect cable response predictions. For example, compared with the responses obtained from case 4 ground motions with those from case 11 motions, assuming homogeneous firm site condition in the analysis may lead to about 50% and 25% underestimations of the mean maximum vertical displacements and axial forces in the transmission line, respectively. As shown in Fig. 22, case 11 ground motions result in the largest cable displacement of 190 cm at one-third span of the transmission line, which have special attention to be paid in establishing the minimum separation distance between transmission lines. Although the softer sites are assumed in case 11, the displacement and axial force responses induced by spatial ground motions of case 11 are relatively insignificant as compared to those of case 10 motions. This is because the greater difference between the soil conditions in case 10 results in the larger phase delay due to the different shear wave velocities in the different soil sites, which can be considered as another wave passage effect, and will induce a further increase in the structural responses.

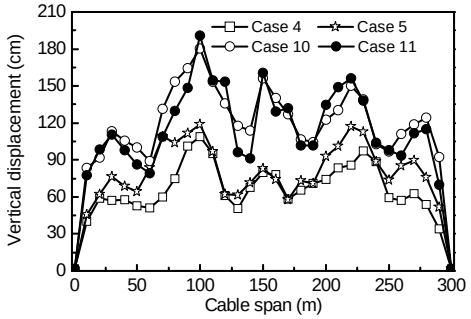

Fig. 22 Mean maximum vertical cable displacements induced by motions considering different soil conditions

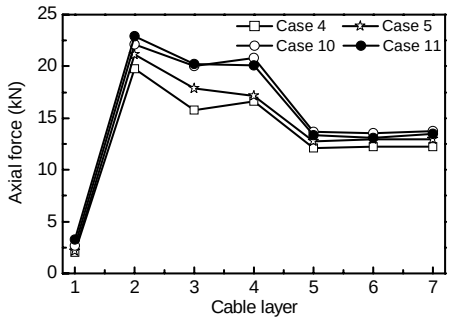

Fig. 23 Mean maximum cable axial forces induced by motions considering different soil conditions

5.4.2 Seismic response of transmission towers

Fig. 24 shows the mean maximum axial forces in tower members along the height of the middle tower induced by spatial ground motions considering different soil condition sets. The responses of tower members corresponding to heterogeneous soil conditions are different from those considering homogeneous soil conditions as well as their larger axial force values. Neglecting the local site effect in the analysis could lead to about 35% underestimation of the mean maximum axial forces in the tower. It is also obvious that although assuming the softer site condition in general leads to overestimation of the structural responses, it may also result in some underestimation of the member axial forces in the upper half of tower. This is again because the greater difference between the soil conditions causes more pronounced ground motion spatial variations.

These observations indicate that the structural responses are amplified by considering the local site effect. Not only the local site condition but also the difference between the soil conditions could influence the seismic response of the structural system. Therefore, it is important to consider the local site effect on ground motion spatial variations in response analysis and design of long span transmission tower-line systems.

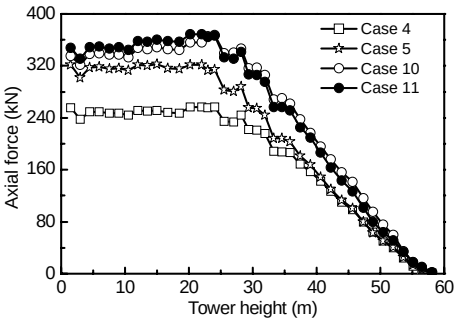

Fig. 24 Mean maximum axial forces in tower members induced by motions considering different soil conditions

6 Conclusions

This paper investigates the seismic responses of a coupled transmission tower-line system at a canyon site subjected to spatially varying ground motions. Each effect of ground motion spatial variations on the responses of the structural system is examined in detail. Based on the numerical results, the following conclusions are drawn:

1. The ground motion spatial variations have a significant effect on seismic responses of transmission tower-line systems. Neglecting ground motion spatial variations in analysis may lead to incorrect predictions of structural responses.

2. The ground motion spatial variations induced by the wave propagation (phase delay) and loss of coherency are important to structural responses. In order to obtain a reliable seismic analysis of the structure, an accurate estimation of wave apparent velocity and coherency loss of the site is necessary.

3. The ground motion spatial variations induced by the heterogeneous site conditions also have significant influences on structural responses. The greater the difference between the soil conditions, the larger structural responses induced. Although the softer site condition assumption in general leads to overestimation of structural responses, it may lead to underestimation of responses in some tower members when the structure is supported on sites of different conditions.

4. A proper seismic design of transmission tower-line systems should consider the influence of wave passage, coherency loss, and local site effects, simultaneously. The analytical results in this paper are applicable to the seismic design for additional coupled transmission tower-line systems owing to common structural dynamic characteristics.

References

Ang, A.H.S., Pires, J.A., Villaverde, R., 1996. A model for the seismic reliability assessment of electric power transmission systems. *Reliability Engineering and System Safety*, **51**(1):7-22. [doi:10.1016/0951-8320(95)00101-8]

ASCE, 1982. American society of civil engineers committee on electrical transmission structures, loadings for electrical transmission structures. *Journal of Structural Division*, **108**(5):1088-1105.

ASCE, 1991. Guideline for Electrical Transmission Line Structural Loading. ASCE Manuals and Reports on Engineering Practice, New York, No. 74.

Ates, S., Dumanoglu, A.A., Bayraktar, A., 2005. Stochastic response of seismically isolated highway bridges with friction pendulum systems to spatially varying earthquake ground motions. *Engineering Structures*, **27**(13):1843-1858. [doi:10.1016/j.engstruct.2005.05.016]

Bai, F.L., Hao, H., Li, H.N., 2009. Response Analysis of a Transmission Tower-Line System to Spatial Ground Motions. Australian Earthquake Engineering Society Conference, Newcastle, Australia.

Der Kiureghian, A., 1980. Structural response to stationary excitation. *Journal of Engineering Mechanics*, **106**(6): 1195-1213.

Dumanoglu, A.A., Soyluk, K., 2003. A stochastic analysis of long span structures subjected to spatially varying ground motions including the site-response effect. *Engineering Structures*, **25**(10):1301-1310. [doi:10.1016/S0141-0296(03)00080-4]

EERI, 1999. Chi-Chi, Taiwan, Earthquake Reconnaissance Report. Earthquake Engineering Research Institute, Oakland, California.

Ghobarah, A., Aziz, T.S., El-Attar, M., 1996. Response of transmission lines to multiple support excitation. *Engineering Structures*, **18**(12):936-946. [doi:10.1016/S0141-0296(96)00020-X]

Hao, H., 1989. Effects of Spatial Variation of Ground Motions on Large Multiply-Supported Structures. Report No. UCB/EERC-89-06, University of California, Berkeley, USA.

Hao, H., 1993. Arch responses to correlated multiple excitations. *Earthquake Engineering and Structural Dynamics*, **22**(5):389-404. [doi:10.1002/eqe.4290220503]

Hao, H., Duan, X.N., 1996. Multiple excitation effects on response of symmetric buildings. *Engineering Structures*, **18**(9):732-740. [doi:10.1016/0141-0296(95)00217-0]

Hao, H., Chouw, N., 2006. Modeling of Earthquake Ground Motion Spatial Variation on Uneven Sites with Varying Soil Conditions. The 9th International Symposium on Structural Engineering for Young Experts, Fuzhou-Xiamen, China, p.79-85.

Hao, H., Oliveira, C.S., Penzien, J., 1989. Multiple-station ground motion processing and simulation based on smart-1 array data. *Nuclear Engineering and Design*, **111**(3):293-310. [doi:10.1016/0029-5493(89)90241-0]

Harichandran, R.S., Hawwari, A., Sweiden, B.N., 1996. Response of long-span bridges to spatially varying ground motion. *Journal of Structural Engineering, ASCE*, **122**(5):476-484. [doi:10.1061/(ASCE)0733-9445(1996)122:5(476)]

Jennings, P.C., Housner, G.W., Tsai, N.C., 1968. Simulated Earthquake Motions. Report of Earthquake Engineering Research Laboratory, EERL-02, California Institute of Technology, USA.

Kawashima, K., Unjoh, S., 1996. Impact of Hanshin/Awaji earthquake on seismic design and seismic strengthening of highway bridges. *Structural Engineering/Earthquake Engineering, JSCE*, **13**(2):211-240.

Li, H.N., Bai, H.F., 2006. High-voltage transmission tower-line system subjected to disaster loads. *Progress in Natural Science*, **16**(9):899-911. [doi:10.1080/10020070612330087]

Li, H.N., Shi, W.L., Wang, G.X., Jia, L.G., 2005. Simplified models and experimental verification for coupled transmission tower-line system to seismic excitations. *Journal of Sound and Vibration*, **286**(3):569-585. [doi:10.1016/j.jsv.2004.10.009]

Moustafa, A., Takewaki, I., 2009. Use of probabilistic and deterministic measures to identify unfavorable earthquake records. *Journal of Zhejiang University-SCIENCE A*, **10**(5):619-634. [doi:10.1631/jzus.A0930001]

Mozer, J.D., Pohlman, J.C., Fleming, J.F., 1977. Longitudinal load analysis of transmission line systems. *IEEE Transactions on Power Apparatus and Systems*, **96**(5):1657-1665. [doi:10.1109/T-PAS.1977.32495]

Nazmy, A.S., Abdel-Ghaffar, A.M., 1987. Seismic Response Analysis of Cable-Stayed Bridges Subjected to Uniform and Multiple-Support Excitations. Report No. 87-SM-1, Department of Civil Engineering, Princeton University, Princeton, NJ, USA.

Nazmy, A.S., Abdel-Ghaffar, A.M., 1992. Effects of ground motion spatial variability on the response of cable-stayed bridge. *Earthquake Engineering and Structural Dynamics*, **22**(1):1-20. [doi:10.1002/eqe.4290210101]

Rassem, M., Ghobarah, A., Heidebrecht, A.C., 1996. Site effects on the seismic response of a suspension bridge. *Engineering Structures*, **18**(5):363-370. [doi:10.1016/0141-0296(95)00001-1]

Ruiz, P., Penzien, J., 1969. Probabilistic Study of the Behaviour of Structures during Earthquakes. Report No. UCB/EERC-69-03, Earthquake Engineering Research Centre, University of California, Berkeley, USA.

Sextos, A.G., Pitilakis, K.D., Kappos, A.J., 2003a. Inelastic dynamic analysis of RC bridges accounting for spatial variability of ground motion, site effects and soil-structure interaction phenomena. Part 1: Methodology and analytical tools. *Earthquake Engineering and Structure Dynamics*, **32**(4):607-627. [doi:10.1002/eqe.241]

Sextos, A.G., Kappos, A.J., Pitilakis, K.D., 2003b. Inelastic dynamic analysis of RC bridges accounting for spatial variability of ground motion, site effects and soil-structure interaction phenomena. Part 2: Parametric study. *Earthquake Engineering and Structure Dynamics*, **32**(4):629-652. [doi:10.1002/eqe.242]

Shen, S.Z., Xu, C.B., Zhao, C., 1997. Design of Suspension Structure. China Architecture and Building Press, Beijing (in Chinese).

Soyluk, K., Dumanoglu, A.A., 2000. Comparison of asynchronous and stochastic dynamic response of a cable-stayed bridge. *Engineering Structures*, **22**(5):435-445. [doi:10.1016/S0141-0296(98)00126-6]

Tajimi, H., 1960. A Statistical Method of Determining the Maximum Response of a Building Structure during an Earthquake. Proceedings of 2nd World Conference on Earthquake Engineering, Tokyo, p.781-796.

Yang, L., Sun, B., Ye, Y., 1996. Calculation of high-voltage

transmission tower. *Engineering Mechanics*, **13**(1):46-51.

Yue, M.G., Li, H.N., Wang, D.S., Zhai, T., 2006. Longitudinal response of the power transmission tower-cable system under travelling seismic wave excitations. *Proceedings of the CSEE*, **26**(23):145-150 (in Chinese).

Zanardo, G., Hao, H., Modena, C., 2002. Seismic response of multi-span simply supported bridges to spatially varying earthquake ground motion. *Earthquake Engineering and Structural Dynamics*, **31**(6):1325-1345. [doi:10.1002/eqe.166]